Time-Optimal Transfer of the Quantum State in Long Qubit Arrays

Andrei A. Stepanenko,[1,2,*] Kseniia S. Chernova,[2] and Maxim A. Gorlach[2,†]
[1]London Institute for Mathematical Sciences, Royal Institution, London, United Kingdom
[2]School of Physics and Engineering, ITMO University, Saint Petersburg 197101, Russia

(Received 29 January 2025; accepted 10 June 2025; published 2 July 2025)

Recent technological advances have allowed the fabrication of large arrays of coupled qubits, serving as prototypes for quantum processors. However, the optimal control of such systems remains notoriously challenging, limiting the potential of large-scale quantum systems. Here, we investigate a model problem of quantum state transfer in a large nearest-neighbor-coupled qubit array. We derive an optimal control strategy that simultaneously achieves maximal fidelity and minimal transfer time, reaching the quantum speed limit in a lattice with time-varying couplings.

DOI: 10.1103/mxrq-7rl4

Introduction—Rapid progress in quantum technologies has enabled large-scale quantum systems capable of performing quantum algorithms and quantum simulations. Existing platforms include trapped ions [1–3], cold atoms [4], photonic systems [5,6], as well as arrays of superconducting qubits [7–12]. Recently, there has been significant growth in the capabilities of these noisy intermediate-scale quantum systems [13,14], accompanied by active discussions of the quantum supremacy concept [7,8,12,15,16].

To fully harness the scale of modern quantum systems, it is important to achieve their complete and flexible control. Therefore, strategies of quantum optimal control [17,18] are under active investigation. Popular approaches include counteradiabatic driving [19–21], shortcuts to adiabaticity [22,23], as well as the quantum brachistochrone method [24–28], which utilizes a geometric approach [26,29].

The quantum brachistochrone technique is based on a variational formulation that aims to minimize the time of the transition between the prescribed quantum states given the constraints on the system's Hamiltonian. This approach has a geometric interpretation in terms of geodesics [26] and yields a tractable system of differential equations [25], which can be solved analytically for relatively simple quantum systems with few degrees of freedom. However, the direct application of this or any other method to large-scale quantum systems is challenging due to the overwhelming number of degrees of freedom and the extremely large parameter space.

In this Letter, we make a conceptual step toward solving this problem. As a physically motivated example, we consider an array of N nearest-neighbor-coupled qubits, assuming that the couplings $J_m(t)$ between them can be tailored on demand and controlled in real time, while the overall sum $\sum_m J_m^2(t)$ is bounded by the constant value J_0^2 [Fig. 1]. Although challenging, such real-time control of couplings is technically feasible. For instance, in superconducting architecture, this could be achieved by inserting auxiliary off-resonant qubits. The change of their eigenfrequencies renormalizes the effective couplings J_m [30,31]. For clarity, we neglect the effects of dissipation and decoherence, focusing on the control of a Hermitian system. As the simplest protocol relevant for quantum communication, we consider the transfer of a single excitation, initiated in the first (leftmost) qubit, to the Nth (rightmost) position. Using a suitable modification of the quantum brachistochrone approach, we derive the optimal control for this system, enabling minimal transfer time and defining the quantum speed limit [32] in a nearest-neighbor coupled lattice with time-varying couplings with a fixed sum $\sum_m J_m^2$. Interestingly, the transfer time scales linearly with the length N of the array, correlating with the

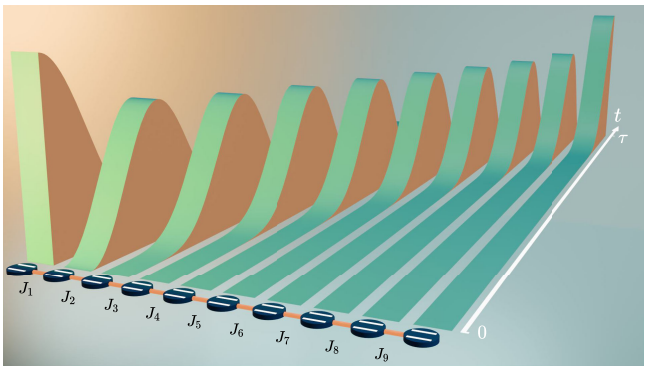

FIG. 1. An artistic view of a single-particle transfer under the time-optimal control of couplings $J_m(t)$ in an array of $N = 10$ coupled qubits. The qubits are depicted by the dark blue cylinders.

*Contact author: as@lims.ac.uk
†Contact author: m.gorlach@metalab.ifmo.ru

results for quantum spin chains [33] and aligning with the intuitive picture of a Gaussian-type wave packet traveling through the array at the highest possible speed.

We model the array of qubits with a Hamiltonian

$$\hat{H} = \sum_m J_m(t)\left(\hat{a}_m^\dagger \hat{a}_{m+1} + \hat{a}_{m+1}^\dagger \hat{a}_m\right), \tag{1}$$

where $\hat{a}_m$ is an annihilation operator in the m th qubit and Planck's constant $\hbar$ is set to unity for simplicity. We also assume that the eigenfrequencies of all qubits are identical, such that the term $\sum_m \omega_m \hat{a}_m^\dagger \hat{a}_m$ contributes only to a constant energy shift, which does not affect the transfer process and is therefore omitted in Eq. (1) for clarity.

The Hamiltonian Eq. (1) commutes with the total number of excitations $\hat{n} = \sum_m \hat{a}_m^\dagger \hat{a}_m$: $[\hat{H}, \hat{n}] = 0$. As a result, the number of excitations is conserved, and the N-dimensional single-particle sector, spanned by the basis vectors $|m\rangle = \hat{a}_m^\dagger |0\rangle$, is decoupled from the full 2^N-dimensional Hilbert space of the system. This reduces the complexity of the problem, allowing us to present the Hamiltonian as the $N \times N$ Hermitian matrix.

Quantum brachistochrone method and governing equations—To find an optimal strategy for switching the couplings $J_m(t)$, we adapt the quantum brachistochrone method [24–26,28]. We introduce the evolution operator $\hat{U}(t)$, which connects the states of the system at two distinct times as $|\psi(t)\rangle = \hat{U}(t)|\psi(0)\rangle$ and satisfies Schrödinger equation

$$i\partial_t \hat{U} = \hat{H}(t)\hat{U}. \tag{2}$$

Since $\mathrm{Tr}\,\hat{H} = 0$ at all times, the Hamiltonian of the array belongs to the (N^2-1)-dimensional space of zero-trace Hermitian matrices. Of these, $(N-1)$ matrices $\hat{A}_n = (\hat{a}_n^\dagger \hat{a}_{n+1} + \hat{a}_{n+1}^\dagger \hat{a}_n)/\sqrt{2}$ describe the coupling of neighboring sites, spanning the subspace $\mathcal{A}$. The remaining (N^2-N) matrices, $\hat{B}_l \in \mathcal{B}$, account for the complex Hermitian couplings and long-range interactions, which are absent in our system. The introduced matrices are normalized by the conditions $\mathrm{Tr}(\hat{A}_m \hat{A}_n) = \delta_{mn}$, $\mathrm{Tr}(\hat{B}_k \hat{B}_l) = \delta_{kl}$, $\mathrm{Tr}(\hat{A}_m \hat{B}_k) = 0$.

We aim to minimize the transfer time τ, given a fixed bound J_0^2 on the sum of squares of the couplings. Although this can be done directly [24,25,34], there is an equivalent, but simpler formulation that seeks to minimize $J_0 = \sqrt{\sum_n J_n^2}$ for a fixed time of the transfer τ. In turn, the sum $2\sum_n J_n^2$ can be recast as $\mathrm{Tr}\,\hat{H}^2 \equiv ||\hat{H}||^2$, resulting in the cost functional $S_0 = \int_0^\tau ||\hat{H}(t)||dt$.

If the Hamiltonian were unrestricted, the best possible strategy would be to couple the initial $|\psi_0\rangle$ and target $|\psi_1\rangle$ state directly by the maximal possible coupling [24]. However, in our case, the Hamiltonian includes only nearest-neighbor couplings, which prevent the direct transfer from the first to the Nth qubit. Therefore, we introduce an additional contribution $S_1 = \int_0^\tau \mathrm{Tr}(\hat{D}\,\hat{H})dt$, where $\hat{D} = \sum_l \lambda_l \hat{B}_l$ contains the matrices from the $\mathcal{B}$ subspace, and λ_l are time-dependent Lagrange multipliers ensuring that the Hamiltonian at any moment of time does not contain any of the $\hat{B}_l$ matrices: $\mathrm{Tr}(\hat{H}\hat{B}_l) = 0$.

Finally, we add two boundary terms to ensure that the state $|\psi_0\rangle$ in the initial moment $t = 0$ is transferred to the target state $|\psi_1\rangle e^{i\phi}$ at $t = \tau$, where the global phase ϕ is irrelevant. Hence, the overall cost functional takes the form

$$\begin{aligned} S = &\int_0^\tau ||\hat{H}(t)||dt + \int_0^\tau \mathrm{Tr}(\hat{D}\,\hat{H})dt \\ &+ \int_0^\tau \mathrm{Tr}\left(\hat{R}_0(\hat{U}\hat{P}_0\hat{U}^\dagger - \hat{P}_0)\right)\delta(t)dt \\ &+ \int_0^\tau \mathrm{Tr}\left(\hat{R}_1(\hat{U}\hat{P}_0\hat{U}^\dagger - \hat{P}_1)\right)\delta(t-\tau)dt, \end{aligned} \tag{3}$$

where $\hat{R}_0$ and $\hat{R}_1$ are the matrices of Lagrange multipliers, and $\hat{P}_{0,1}$ matrices project on the initial and target states of the system as $\hat{P}_0 = |\psi_0\rangle\langle\psi_0|$, $\hat{P}_1 = |\psi_1\rangle\langle\psi_1|$.

Since the Hamiltonian is expressed in terms of $\hat{U}$ as $\hat{H} = i(\partial_t \hat{U})\hat{U}^\dagger$, the above functional depends on the evolution operator $\hat{U}(t)$, its time derivative, and the Lagrange multipliers λ_l, $\hat{R}_0$, $\hat{R}_1$. Varying with respect to $\hat{U}$ and requiring $\delta S = 0$, we derive the quantum brachistochrone equation [25,26,28]

$$\partial_t(\hat{H} + \hat{D}) + i[\hat{H}, \hat{D}] = 0, \tag{4}$$

which defines the change of the Hamiltonian in time. An immediate consequence of Eq. (4) is

$$\mathrm{Tr}\,\hat{D} = \mathrm{const}, \tag{5}$$

where the constant on the right-hand side is determined by the initial conditions.

However, finding the optimal protocol from Eq. (4) is generally a challenging task, since the initial conditions for the couplings $J_m(0)$ and the Lagrange multipliers $\lambda_l(0)$ are unknown. For small-scale quantum systems, this issue can be overcome by defining the evolution operator at the initial and final moments of time and solving the resulting boundary value problem either analytically or by the shooting method [25]. Further improvement is obtained by relating the solutions of Eq. (4) to the geodesics in space with a special metric [26]. Here, we take a different approach and derive the boundary conditions by varying the two terms of S with the delta function:

$$\hat{H}(0) + \hat{D}(0) = -i[\hat{P}_0, \hat{R}_0], \tag{6}$$

$$\hat{H}(\tau) + \hat{D}(\tau) = i[\hat{P}_1, \hat{R}_1]. \tag{7}$$

Some of the scalar equations in the system (6) and (7) are independent of $\hat{R}_0$ and $\hat{R}_1$ components, and those provide the boundary conditions of interest. This formulation of quantum brachistochrone Eqs. (4)–(7) significantly simplifies the calculation, as we have to seek not the entire matrix of the evolution operator with N^2 components, but rather the wave function $|\psi\rangle$ with only N entries solving the Schrödinger equation

$$i\frac{\partial|\psi\rangle}{\partial t} = \hat{H}|\psi\rangle \tag{8}$$

with $2N-1$ initial and boundary conditions for the wave function:

$$\psi_n(0) = \delta_{n1}, \qquad \psi_k(\tau) = 0, \tag{9}$$

where $n = 1, \ldots, N$ and $k = 1, \ldots, N-1$.

Control algorithm—To proceed with the solution, we choose a specific basis in the (N^2-1)-dimensional space of traceless Hermitian matrices. To that end, we introduce a matrix function

$$\hat{X}_{mn}(z) = \frac{1}{\sqrt{2}}(zE_{nm} + z^*E_{mn}), \tag{10}$$

where z is an arbitrary complex number and E_{nm} is a matrix with the elements $(E_{nm})_{pq} = \delta_{np}\delta_{mq}$. In these notations, $\hat{A}_m = \hat{X}_{m,m+1}(1)$. In turn, the matrices from the $\mathcal{B}$ subspace are constructed as $\hat{B}^e_{m,m+q} = \hat{X}_{m,m+q}(i^{q-1})$ for $1 < q \leq N-m$, $\hat{B}^o_{m,m+q} = \hat{X}_{m,m+q}(i^q)$ for $1 \leq q \leq N-m$, and $\hat{B}_{m,m} = (\sum_{p=1}^{m} E_{pp} - mE_{m+1,m+1})\sqrt{2/(m^2+m)}$ where $1 \leq m < N$. This choice of the matrices provides a slight modification of the generalized Gell-Mann matrices [35].

In such a basis, the quantum brachistochrone equation, Eq. (4), results in a set of scalar equations [36]

$$\sqrt{2}\partial_t J_m = J_{m+1}\lambda_{m,m+2} - J_{m-1}\lambda_{m-1,m+1}, \tag{11}$$

$$\begin{aligned}\partial_t\lambda_{k,k+n} = {} & J_{k+n}\lambda_{k,k+n+1} - J_{k-1}\lambda_{k-1,k+n} \\ & - J_{k+n-1}\lambda_{k,k+n-1} + J_k\lambda_{k+1,k+n},\end{aligned} \tag{12}$$

where $2 \leq n \leq N-k$ and $1 \leq k \leq N-2$. Notably, the system only contains Lagrange multipliers $\lambda_{m,m+q}$ corresponding to the matrices $\hat{B}^e_{m,m+q}$, while the terms associated with $\hat{B}^o_{m,m+q}$ and $\hat{B}_{m,m}$ drop out due to the structure of the problem.

Applying the boundary conditions Eqs. (6) and (7), we recover [36] that most of the couplings at the initial moment are zero $J_m(0) = 0$ for $m \neq 1$, while at the final time $J_m(\tau) = 0$ for $m \neq N-1$. This result is very intuitive: to transfer the excitation from the first qubit elsewhere, one has to maximize the coupling J_1 while keeping the rest of the couplings zero.

What is less intuitive is that the majority of the coefficients $\lambda_{k,k+n}$ are also zero at $t = 0$ and $t = \tau$, with the only nonzero coefficients being $\lambda_{1,2+n}(0)$ and $\lambda_{n,N}(\tau)$ for $1 \leq n \leq N-2$.

Thus, our problem has $N(N+1)/2$ unknowns, including N complex components of the wave function $|\psi\rangle$, $(N-1)$ real couplings J_m, and $(N-1)(N-2)/2$ real-valued Lagrange multipliers. These unknowns satisfy the same number of independent differential equations (4) and (8).

This is supplemented by (N^2-N+1) initial and boundary conditions, including $(2N-1)$ conditions for the wave function Eqs. (9) and $(N-1)(N-2)$ conditions for quantum brachistochrone equation [36]. Hence, starting from $N = 3$, the number of conditions exceeds the number of equations, and the system becomes overdetermined. Physically, this reflects the fact that the optimal solution may not exist. However, as we demonstrate below, the optimal solution does exist and is uniquely constructed.

Specifically, we determine $J_1(0)$ and $\lambda_{1,2+n}(0)$ by the shooting method. Importantly, our formulation requires only $(N-1)$ initial conditions for the shooting. As a result, the numerical search for short arrays ($N < 5$) converges to the same result for a practically random initial guess.

The computation becomes more complex for longer arrays. In this case, we proceed iteratively, using the solution for the array with $N-1$ qubits to construct the initial guess for N-qubit problem. The standard shooting method works relatively well on a personal computer for $N < 17$. For longer arrays, we seek $J_1(0)$ and $\lambda_{1,1+q}(0)$ by the gradient optimization method yielding the solution for N as large as 100.

Key results—To illustrate our approach, we compute the optimal control and the associated evolution of the wave function for an array consisting of 15 qubits. Figure 2(a) shows the probability distribution $|\psi_n|^2$ for the quantum state at several representative moments of time. We observe that the excitation propagates in the array as a tightly bound wave packet retaining its shape with modifications occurring only near the boundaries.

On the other hand, by tracking the evolution of the probabilities $|\psi_n|^2$ versus time for various n [Fig. 2(b)], we observe that the curves peak as the wave packet passes the respective site. The curves for different sites n are practically identical up to the shift in time.

Finally, Fig. 2(c) shows the evolution of the quantum state both in space and time. The expectation value of the wave packet's position, shown by the red dashed line, exhibits linear growth over time. For clarity, we compare the derived time-optimal strategy with two alternative scenarios that ensure maximal fidelity of the transfer.

The first approach involves stepwise switching of the couplings. At each time step of duration $\Delta\tau = \pi/(2J_0)$,

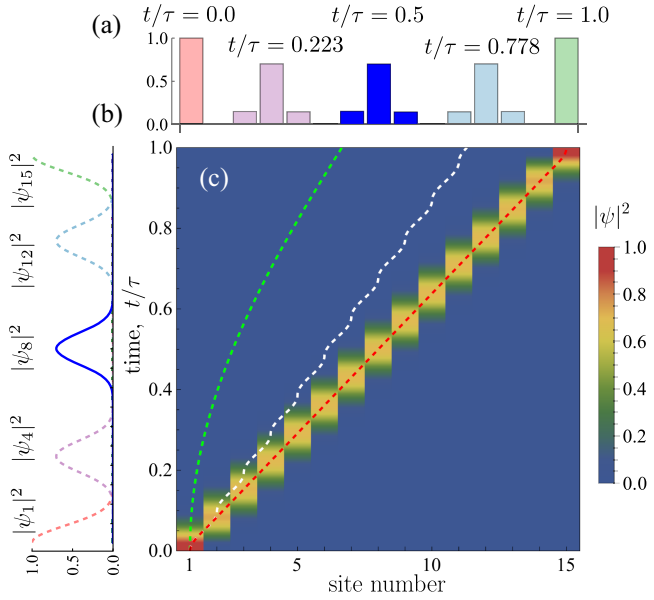

FIG. 2. Numerical results for time-optimal transfer in a 15-qubit array. (a) Histogram showing the instantaneous probability distribution $|\psi_n(t)|^2$ at several representative moments of time. The wave packet remains tightly bound. (b) The dependence of probabilities $|\psi_n(t)|^2$ on time in several selected sites of the lattice. (c) Evolution of the probability distribution in the array during the whole process of the transfer $0 \le t \le \tau$. Lines show the expectation value of the wave packet position for time-optimal control (red), stepwise switching of the couplings (white), and perfect transfer scenario (green line).

only two qubits are coupled with each other. By switching the couplings one after another in this manner, the excitation can be transferred from the first to the Nth qubit within the time

$$\tau_{st} = \frac{(N-1)\pi}{2J_0}. \tag{13}$$

The expectation value of the particle's position as a function of time in this case is shown in Fig. 2(c) by the dashed white line.

Another strategy is to keep all couplings in the array constant over time, but dependent on the coordinate: $J_m = \gamma\sqrt{m(N-m)}/2$. This scenario, known as perfect transfer [37], also ensures maximal fidelity. However, the timing in this case is clearly nonoptimal,

$$\tau_p = \pi/\gamma = \frac{\pi}{J_0}\sqrt{\frac{N(N^2-1)}{24}}, \tag{14}$$

and scales roughly as $N^{3/2}$. This scenario is illustrated in Fig. 2(c) by the dashed green line. Notably, both scenarios are significantly slower compared to our time-optimal solution [Fig. 2(c)].

Having an efficient numerical procedure to solve quantum brachistochrone equations, we now analyze the scaling of the transfer time with the length N of the array [Fig. 3(a)]. In our calculations, we examine sufficiently large qubit arrays, with N reaching state-of-the-art levels of 100 [12]. Our results suggest that the transfer time scales linearly with the length N, which agrees with the intuitive picture of a wave packet propagating at the maximal possible speed while retaining its spatial profile. The dependence of the transfer time on N is well approximated by

$$\tau(N) = (1.13045N - 0.6677)/J_0. \tag{15}$$

This asymptotic formula is valid for the sufficiently large N and slightly underestimates the transfer time having an absolute error of 0.0003 for $N = 10$.

We compare these results with the two alternative approaches summarized above. Stepwise switching of the couplings [Eq. (13)] also provides a linear scaling, but the time of the transfer in the limit $N \to \infty$ is 39% higher than for our solution. Even poorer results are obtained for time-independent couplings (the "perfect transfer" scenario), where the transfer time Eq. (14) scales as $N^{3/2}$. This comparison highlights the potential of optimal control for large-scale quantum systems, providing an optimization of standard tasks such as quantum state transfer.

However, finding the optimal control for large quantum systems is not always straightforward. In our case, a clue to the efficient numerical solution is provided by the behavior of $\lambda_{1,1+p}(0)$ coefficients ($2 \le p \le N-1$), whose dependence on the length of the array rapidly saturates as N exceeds 10, reflecting the localized nature of the solution. At the same time, the dependence on p is relatively weak [Fig. 3(b)]. Hence, having a solution for the array of N qubits, we can construct an initial guess for a longer array improving it by the gradient optimization.

Inspecting the robustness of the derived protocol to the random disorder in the couplings, we observe that it is significantly more robust than the perfect transfer strategy and features comparable robustness as the stepwise switching scenario [36].

To conclude, our work derives an example of time-optimal control for a large-scale array of nearest-neighbor-coupled qubits. Despite its conceptual simplicity, our model embodies the features of present-day superconducting quantum processors and demonstrates ways to significantly enhance their performance through the use of optimal control strategies. As we prove, the quantum brachistochrone technique combined with suitable numerical algorithms provides a significant speed-up of quantum state transfer compared to more traditional approaches and allows us to derive the quantum speed limit in a lattice with time-varying couplings.

We believe that this study will stimulate further advances in quantum communication, as well as in a broader realm of quantum physics, e.g., in connection to time-optimal

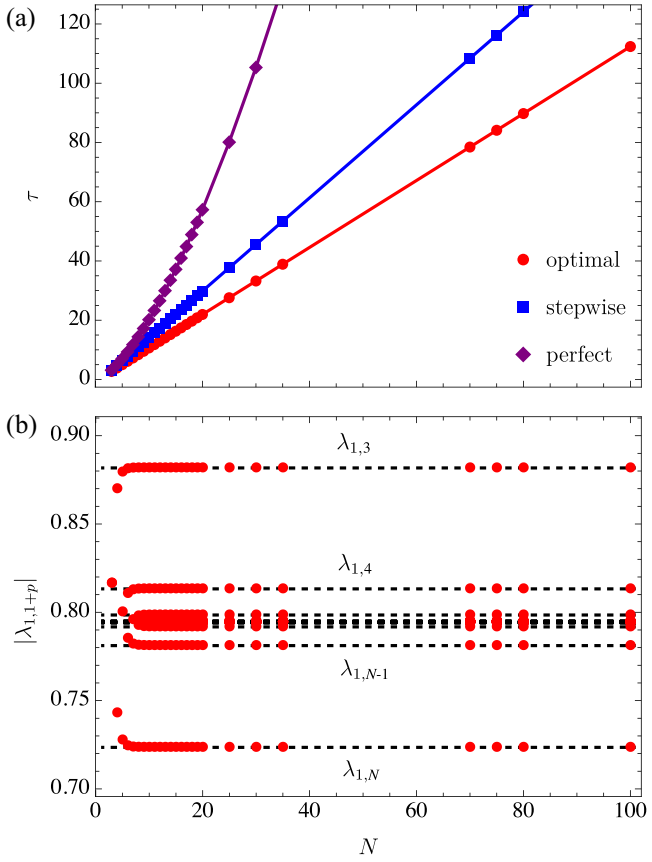

FIG. 3. Scaling of the transfer time and parameters of numerical solution with the length N of the array. (a) Transfer time versus the length of the array for time-optimal control (circles), stepwise switching of the couplings (squares), and perfect transfer (rhombs). (b) Initial values of $\lambda_{1,1+p}$ parameters used in numerical solution. Black dashed line shows projected asymptotic values in the limit $N \to \infty$. We set $J_0 = 1$.

generation of high harmonics or nonclassical states of light [38,39].

Acknowledgments—We acknowledge D. Stepanenko for help with illustrations. We thank A. Gorlach, O. Gamayun, A. Fedorov, S. Kilin, D. Mogilevtsev, and A. Mikhalychev for valuable discussions. Theoretical models were supported by Priority 2030 Federal Academic Leadership Program. Numerical simulations were supported by the Russian Science Foundation, Grant No. 24-72-10069. M. A. G. acknowledges partial support by the Foundation for the Advancement of Theoretical Physics and Mathematics "Basis."

Data availability—The data supporting this study's findings are available within the Letter.

[1] C. D. Bruzewicz, J. Chiaverini, R. McConnell, and J. M. Sage, Trapped-ion quantum computing: Progress and challenges, Appl. Phys. Rev. **6**, 021314 (2019).

[2] S. Moses, C. Baldwin, M. Allman *et al.*, A race-track trapped-ion quantum processor, Phys. Rev. X **13**, 041052 (2023).

[3] J.-S. Chen, E. Nielsen, M. Ebert *et al.*, Benchmarking a trapped-ion quantum computer with 30 qubits, Quantum **8**, 1516 (2024).

[4] D. Bluvstein, S. J. Evered, A. A. Geim *et al.*, Logical quantum processor based on reconfigurable atom arrays, Nature (London) **626**, 58 (2023).

[5] L. S. Madsen, F. Laudenbach, M. F. Askarani *et al.*, Quantum computational advantage with a programmable photonic processor, Nature (London) **606**, 75 (2022).

[6] C. Taballione, M. C. Anguita, M. de Goede *et al.*, 20-mode universal quantum photonic processor, Quantum **7**, 1071 (2023).

[7] F. Arute, K. Arya, R. Babbush *et al.*, Quantum supremacy using a programmable superconducting processor, Nature (London) **574**, 505 (2019).

[8] Y. Wu, W.-S. Bao, S. Cao *et al.*, Strong quantum computational advantage using a superconducting quantum processor, Phys. Rev. Lett. **127**, 180501 (2021).

[9] S. Bravyi, O. Dial, J. M. Gambetta, D. Gil, and Z. Nazario, The future of quantum computing with superconducting qubits, J. Appl. Phys. **132**, 160902 (2022).

[10] A. Anferov, S. P. Harvey, F. Wan, J. Simon, and D. I. Schuster, Superconducting qubits above 20 GHz operating over 200 mK, PRX Quantum **5**, 030347 (2024).

[11] A. Morvan, B. Villalonga, X. Mi *et al.*, Phase transitions in random circuit sampling, Nature (London) **634**, 328 (2024).

[12] R. Acharya, D. A. Abanin, L. Aghababaie-Beni *et al.*, Quantum error correction below the surface code threshold, Nature (London) **638**, 920 (2024).

[13] J. Preskill, Quantum Computing in the NISQ era and beyond, Quantum **2**, 79 (2018).

[14] K. Bharti, A. Cervera-Lierta, T. H. Kyaw, T. Haug, S. Alperin-Lea, A. Anand, M. Degroote, H. Heimonen, J. S. Kottmann, T. Menke, W.-K. Mok, S. Sim, L.-C. Kwek, and A. Aspuru-Guzik, Noisy intermediate-scale quantum algorithms, Rev. Mod. Phys. **94**, 015004 (2022).

[15] F. Pan, K. Chen, and P. Zhang, Solving the sampling problem of the Sycamore quantum circuits, Phys. Rev. Lett. **129**, 090502 (2022).

[16] J. F. F. Bulmer, B. A. Bell, R. S. Chadwick, A. E. Jones, D. Moise, A. Rigazzi, J. Thorbecke, U.-U. Haus, T. Van Vaerenbergh, R. B. Patel, I. A. Walmsley, and A. Laing, The boundary for quantum advantage in Gaussian boson sampling, Sci. Adv. **8**, eabl9236 (2022).

[17] J. Werschnik and E. K. U. Gross, Quantum optimal control theory, J. Phys. B **40**, R175 (2007).

[18] U. Boscain, M. Sigalotti, and D. Sugny, Introduction to the Pontryagin maximum principle for quantum optimal control, PRX Quantum **2**, 030203 (2021).

[19] M. Demirplak and S. A. Rice, Adiabatic population transfer with control fields, J. Phys. Chem. A **107**, 9937 (2003).

[20] M. V. Berry, Transitionless quantum driving, J. Phys. A **42**, 365303 (2009).

[21] F. M. D'Angelis, F. A. Pinheiro, D. Guéry-Odelin, S. Longhi, and F. Impens, Fast and robust quantum state transfer in a topological Su-Schrieffer-Heeger chain with

next-to-nearest-neighbor interactions, Phys. Rev. Res. **2**, 033475 (2020).
[22] A. del Campo, Shortcuts to adiabaticity by counterdiabatic driving, Phys. Rev. Lett. **111**, 100502 (2013).
[23] D. Guéry-Odelin, A. Ruschhaupt, A. Kiely, E. Torrontegui, S. Martínez-Garaot, and J. G. Muga, Shortcuts to adiabaticity: Concepts, methods, and applications, Rev. Mod. Phys. **91**, 045001 (2019).
[24] A. Carlini, A. Hosoya, T. Koike, and Y. Okudaira, Time-optimal quantum evolution, Phys. Rev. Lett. **96**, 060503 (2006).
[25] A. Carlini, A. Hosoya, T. Koike, and Y. Okudaira, Time-optimal unitary operations, Phys. Rev. A **75**, 042308 (2007).
[26] X. Wang, M. Allegra, K. Jacobs, S. Lloyd, C. Lupo, and M. Mohseni, Quantum brachistochrone curves as geodesics: Obtaining accurate minimum-time protocols for the control of quantum systems, Phys. Rev. Lett. **114**, 170501 (2015).
[27] D. Wang, H. Shi, and Y. Lan, Quantum brachistochrone for multiple qubits, New J. Phys. **23**, 083043 (2021).
[28] S. Malikis and V. Cheianov, Integrability and chaos in the quantum brachistochrone problem, Phys. Rev. A **110**, 022205 (2024).
[29] C. V. Meinersen, S. Bosco, and M. Rimbach-Russ, Quantum geometric protocols for fast high-fidelity adiabatic state transfer, arXiv:2409.03084.
[30] R. Keil, C. Poli, M. Heinrich, J. Arkinstall, G. Weihs, H. Schomerus, and A. Szameit, Universal sign control of coupling in tight-binding lattices, Phys. Rev. Lett. **116**, 213901 (2016).
[31] I. N. Moskalenko, I. A. Simakov, N. N. Abramov, A. A. Grigorev, D. O. Moskalev, A. A. Pishchimova, N. S. Smirnov, E. V. Zikiy, I. A. Rodionov, and I. S. Besedin, High fidelity two-qubit gates on fluxoniums using a tunable coupler, npj Quantum Inf. **8**, 130 (2022).
[32] S. Deffner and S. Campbell, Quantum speed limits: From Heisenberg's uncertainty principle to optimal quantum control, J. Phys. A **50**, 453001 (2017).
[33] M. Murphy, S. Montangero, V. Giovannetti, and T. Calarco, Communication at the quantum speed limit along a spin chain, Phys. Rev. A **82**, 022318 (2010).
[34] J. Yang and A. del Campo, Minimum-time quantum control and the quantum brachistochrone equation, arXiv:2204.12792.
[35] R. A. Bertlmann and P. Krammer, Bloch vectors for qudits, J. Phys. A **41**, 235303 (2008).
[36] See Supplemental Material at http://link.aps.org/supplemental/10.1103/mxrq-7rl4 for the derivation of quantum brachistochrone equation, derivation of control equations for our problem, tables and graphs illustrating the optimal control for qubit arrays of various lengths, and the analysis of the transfer fidelity versus the strength of random fluctuations of the couplings which includes Refs. [24–26,28,35].
[37] M. Christandl, N. Datta, A. Ekert, and A. J. Landahl, Perfect state transfer in quantum spin networks, Phys. Rev. Lett. **92**, 187902 (2004).
[38] A. Gorlach, O. Neufeld, N. Rivera, O. Cohen, and I. Kaminer, The quantum-optical nature of high harmonic generation, Nat. Commun. **11**, 4598 (2020).
[39] A. Gorlach, M. E. Tzur, M. Birk, M. Krüger, N. Rivera, O. Cohen, and I. Kaminer, High-harmonic generation driven by quantum light, Nat. Phys. **19**, 1689 (2023).